Catalysis Today 164 (2011) 336–340

Contents lists available at ScienceDirect

Catalysis Today

journal homepage: www.elsevier.com/locate/cattod

Dehydrogenation of ethylbenzene to styrene on a direct synthesized Co, Ni/carbon nanotubes catalysts

Xiao-Feng Guo [a], Joong-Ho Kim [b], Geon-Joong Kim [a,*]

[a] Department of Chemical Engineering, Inha University, 253 younghyun-dong, Nam-gu, Inchoen 402-751, Republic of Korea
[b] School of Applied Chemical Engineering, Chonnam National University, Gwangju 500-757, Republic of Korea

ARTICLE INFO

Article history:
Available online 5 November 2010

Keywords:
Dehydrogenation
SBA-15
Carbon nanotubes

ABSTRACT

Multi-walled carbon nanotubes were synthesized by chemical vapor deposition method using SBA-15 as a template under methane and carbon dioxide as carbon sources. As-synthesized multi-walled carbon nanotubes were treated by NaOH at 80 °C to remove the template and retain the Ni and Co metals. The multi-walled carbon nanotubes supported (Co and Ni) were used as catalysts. The catalysts were characterized by SEM, TEM, XRD, Raman and SEM-EDX. The catalytic activity was investigated for the dehydrogenation of ethylbenzene at different oxidants and temperatures. CNTs-Co-10 showed the highest styrene selectivity (92.3%) at 450 °C and ethylbenzene conversion (93.5%) at 700 °C with a higher styrene yield (80.6). The catalyst also showed a high thermal stability.

1. Introduction

Oxidative dehydrogenation of ethylbenzene (ODE) to styrene is an attractive process due to its advantages over the conventional endothermic dehydrogenation reaction [1]. A number of catalysts such as active alumina [2], mixed-oxide [3] and phosphates [4] have been applied as catalysts for ODE, and the accumulated carbon layers deposited on the catalyst surface have been identified as the real active catalysts converting ethylbenzene (EB) to styrene (ST). Therefore, various carbon based materials have been tested as catalysts, providing higher activity and selectivity compared to those as-stated catalysts under mild operating conditions (350–400 °C) [5,6]. However, deactivation of these carbon catalysts becomes a main problem since coke deposition on the catalyst surface changes their initial physico-chemical properties, and since the carbon-based catalysts are relatively sensitive to oxygen. Schlögl and coworkers have conducted studies of ODE on a series of non-planar sp2-nanocarbon materials, such as carbon nanotubes (CNTs), onion-like carbon (OLC) and carbon nanofibers (CNFs) at mostly above 500 °C [7–9]. Several investigators have already demonstrated the microstructure effect of carbon nanofiber on the activity or the selectivity in the special catalytic systems using CNFs supported metal catalysts [10]. Their results showed that a higher and more stable activity could be reached on these nanocarbon materials than that on high surface area graphite and carbon black [7]. The supported carbon nanofibers are also employed as catalysts in ODE, revealing that selectivity to styrene is not significantly affected by the conversion of ethylbenzene [9]. Very recently, Pereira et al. [11] have demonstrated that carbon nanotubes produced by CCVD have a higher stability compared to active carbons during ODE at 450 °C. However, the selectivity to styrene is regarded as the crucial parameter in the catalyst development for ODE due to a small gap in the price between ethylbenzene and styrene [12]. The catalyst selectivity during ODE has been much less addressed in the literature so far, compared to investigations on catalyst activity and stability.

Oxidative dehydrogenation of ethylbenzene on CNTs supported metal catalyst can be considered as a good model system. In our study, we have been involved with the study of CNTs as supports for catalytic reactions. One of the interesting features of these materials is their ability to participate in the catalytic reactions and also function as a high-surface-area support with a high thermal stability. The combination of catalyst and support reactivity has led to synergism in the catalytic activity. Previous studies show that the support materials for the catalysts play a key role in the type of nanotubes produced (such as the number of walls, the diameter, and the graphitization). A good catalyst material for CNTs synthesis necessarily exhibits strong metal support interactions and possesses a high surface area and large pore volume. And it should retain these characteristics at high temperature without sintering. The ordered mesoporous silica materials are excellent catalyst supports because they are mechanically and thermally stable and have strong interactions with metal catalysts such as Fe, Ni, and Co and also because they have a large pore size similar to the diameter of CNTs [13]. Herein, we introduced the Ni or Co inside the pore structure of SBA-15 with two-dimensional (2D) hexagonal mesoporous silica.

* Corresponding author. Tel.: +82 32 860 7472; fax: +82 32 872 4046.
E-mail address: kimgj@inha.ac.kr (G.-J. Kim).

0920-5861/$ – see front matter © 2010 Elsevier B.V. All rights reserved.
doi:10.1016/j.cattod.2010.10.004

SBA-15 containing Co and Ni nanoparticles as catalysts was used to fabricate carbon nanotube. This provides a new, easy method to control the orientation of aligned CNTs by the transition metal catalysts incorporated into ordered mesopores with a molecularly well-defined structure. The open large pore allows efficient diffusion of reactant and intermediate hydrocarbon species and more efficiently promotes nanotube yield and purity [13].

Herein, we synthesized CNTs supported metal directly by chemical vapor deposition (CVD) method using three different Ni or Co/SBA-15 catalysts and using methane and environmental-friendly CO_2 as carbon sources. To synthesize nanotubes with selectivity, and to control the crystallinity of walls and the diameter of the generated nanotubes, the catalytic process has been studied as a function of the Ni or Co content. All the catalysts were employed in the dehydrogenation of ethylbenzene to styrene to test their catalytic activity and selectivity.

2. Experimental details

2.1. Catalyst preparation

A high quality SBA-15 was prepared using the triblock copolymer Pluronic P123 (Aldrich) as a surfactant and tetraethylorthosilicate (TEOS, 98%, Aldrich) as a silica source, modifying the synthetic procedure reported by Zhao et al. [14]. The starting composition in molar ratio for the synthesis of high grade SBA-15 was fixed as 1.72 P123:0.1 TEOS:0.6 HCl:20 H_2O.

The SBA-15 support was impregnated with ethanol solution of nickel or cobalt nitrate at a specific concentration at room temperature for 3 h, evaporated, dried at 100 °C for 12 h. The sample was used to synthesize CNTs without further treatment. The mass fraction of Ni or Co in the Ni or Co/SBA-15 catalyst is in the range of 10–30 wt%.

2.2. Synthesis of CNTs

0.5 g catalyst was put into a quartz tube. The catalyst was pretreated at H_2 at 700 °C for 2 h. It was heated to 900 °C under a CH_4 (200 sccm) and CO_2 flow (200 sccm). After a certain reaction time (60 min), the system was cooled to room temperature under only H_2. Composite of CNTs and Ni or Co-SBA-15 were treated by 80 °C NaOH solution (2 M) for 3 times to remove the template. Samples of CNTs which were prepared by 10 wt% Ni-SBA-15, 30 wt% Ni-SBA-15, 10 wt% Co-SBA-15 and 30 wt% Co-SBA-15 by the reaction of methane and carbon dioxide were designated as CNTs-Ni-10, CNTs-Ni-30, CNTs-Co-10 and CNTs-Co-30, respectively.

2.3. Apparatus and procedure

The reaction was carried out using a flow-type reactor (quartz tube, 20 mm ID, 1 mm OD, 500 mm length) and was operated at atmospheric pressure. A catalyst (3 g) was placed in the center of the reactor using a quartz glass wool plug. The reaction was carried out at 450–700 °C for 1–8 h. When the activated carbon or CNTs supported metal catalysts were used, the catalyst was treated by the following procedure, before introducing ethylbenzene. The catalyst was heat-treated under an argon stream from room temperature to 600 °C and it was maintained at this temperature for 10 min. Then, the catalyst was maintained at the same temperature under an air stream for 10 min, and the reactor was cooled to the desired reaction temperature under a stream of argon. Ethylbenzene was fed (ca. 3 ml/h) to the reactor by passing air, carbon dioxide or argon (30 ml/min) through the ethylbenzene syringe pump preheated at 180 °C. The condensed material was cooled externally in an ice water bath.

2.4. Characterization

X-ray powder diffraction (XRD) data were acquired on a D/MAX 2500 V/PC diffractometer using CuKα radiation. The morphology and microstructures of as-prepared samples were characterized by field emission transmission electron microscopy (FE-TEM, S-4200), and field emission scanning electron microscopy (FE-SEM, JEM-2100F). The nitrogen adsorption/desorption analysis was performed at −196 °C by using a surface area and porosity equipment (Micromeritics, ASAP 2010). The specific surface areas were calculated according to BET theory, and the mean pore size was determined by BJH analysis. Raman Breaker (FT-Raman, RFS-100/S) was used to measure the vibrational properties of the obtained CNTs. Reaction products (ethylbenzene, styrene, toluene and benzene) were analyzed with a gas chromatograph equipped with FID, using a 0.32 mm 30 m glass column packed with HP-5.

3. Results and discussion

A highly ordered SBA-15 was characterized by XRD, SEM, TEM and N_2 adsorption analysis. The ordered arrangement of mesopore in the synthesized SBA-15 gives rise to the well-resolved XRD peaks as shown in Fig. 1, which can be assigned to (1 0 0), (1 1 0), and (2 0 0) diffractions of the 2D hexagonal space group (p6mm). FE-TEM images of SBA-15 viewed along or perpendicular to the direction of hexagonal pore arrangement further confirmed 2D hexagonal structure. FE-SEM images revealed that as-synthesized SBA-15 sample consists of many rope-like domains with relatively uniform sizes of ∼2 μm, which are aggregated into wheat-like macrostructures. N_2 adsorption–desorption isotherms of calcined original SBA-15 are the H1-type hysteresis loop that is typical for mesoporous materials with ordered cylindrical channels.

Fig. 2 shows the influences of metals content on the morphology of CNTs synthesized at 900 °C by the reaction of methane and carbon dioxide. It can be observed that the average diameters of CNTs increase with the rise of nickel and cobalt contents. Most CNTs tangle together and with diameters from 8 to 30 nm. When the cobalt content is 10 wt% in the catalyst, the CNTs diameter is uniform and close to 10 nm, as shown in Fig. 2A and B, and a few impurities can be seen, the wall surfaces of CNTs are clean. But when increasing the metals content to 30 wt%, the CNTs diameters become uneven and the CNTs with large diameter appear (see Fig. 2C, D and G, H), and some impurities containing amorphous carbon can be seen.

The TEM images for the CNTs are shown in Fig. 3. It can be observed that the average diameters of CNTs increase with the rise of metal contents as similar as SEM images. It can be seen that the crooked CNTs with a diameter varied from 8.8 to 16.5, 15 to 19.8 nm with creasing content of Ni from 10 to 30, and Co from 10 to 30 wt%. TEM of CNTs further confirmed the results of SEM. It reveals the multi-walled structure and herringbone graphitic sheets of the CNTs. The average interlayer spacing of 0.35 nm and the sharp strips between the graphitic sheets indicate their good crystallinity. Some section-sealed structure can be observed in the interior of the CNTs in Fig. 3. Particles of Ni and Co on top of CNTs were characterized by TEM. Averaged particle sizes increased from 13.6 nm to 17.8 nm with increasing content of Co from 10 wt% to 30 wt%. Averaged particle sizes were changed from 15.6 to 25 nm with increasing content of Ni from 10 wt% to 30 wt%.

The metal-MWNTs systems have been selected for further investigation. Fig. 4 shows the XRD patterns for CNTs supported Ni and cobalt catalyst. From the two Co patterns at the bottom of Fig. 4A and B, we can see, a hump appears near the strongest diffraction peak of the fcc cobalt at $2\theta = 44.24$. At the same time, three small peaks appeared at 19.1°, 51.5° and 76.1°. The formation of trace carbide Co_2C was found at 37.9°. This indicates that

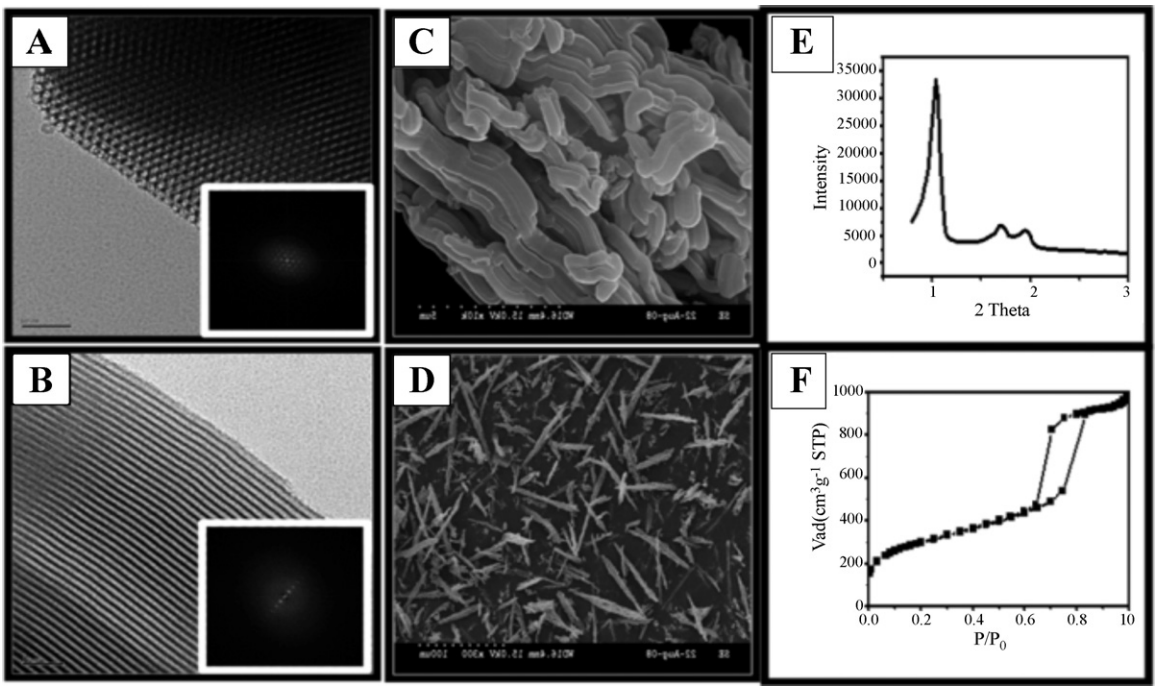

Fig. 1. Characterization of SBA-15: TEM viewed from 1 1 0 (A) and viewed from 0 0 1 (B); SEM at high magnification (C) and low magnification (D); XRD (E) and nitrogen adsorption/desorption isotherm (F).

Co and CNTs are not only dispersed on the surface of CNTs but also formed the Co_2–C bond. In Ni-MWNTs system (two top patterns in Fig. 4), there are three peaks in the X-ray pattern beside the CNTs, which is attributed the Ni metal. The formation of nickel carbide Ni_3C was not obtained in our experiments.

Raman spectroscopy (Fig. 5) was further used to characterize the product, in which a high intense G-band (about 1600 cm^{-1}) and a low intense D-band (about 1280 cm^{-1}) was observed, which indicates the quality and defect of CNTs. The D-band is associated with the amount of disordered carbon and occurs in the 1200–1400 cm^{-1} part of the spectrum. The G-band reveals the intense tangential modes of CNTs and the good arrangement of the hexagonal lattice of graphite which occurs in the high frequency region of 1500–1600 cm^{-1}. G-band of CNTs was decreased slowly with increasing content of metals (Ni and Co).

Metal content of CNTs supported Co and Ni before and after NaOH was analyzed by SEM-EDX. The results are summarized in Table 1. After NaOH treated at 80 °C, content of CNTs-Co-10, CNTs-Co-30, CNTs-Ni-10 and CNTs-Ni-30 were 9.5, 12.6, 9.3 and 13.1 wt% carbon, respectively. It indicated that some metals were removed during NaOH treatment from metal-CNTs system. It may be attributed that high content of Ni and Co can form much bigger

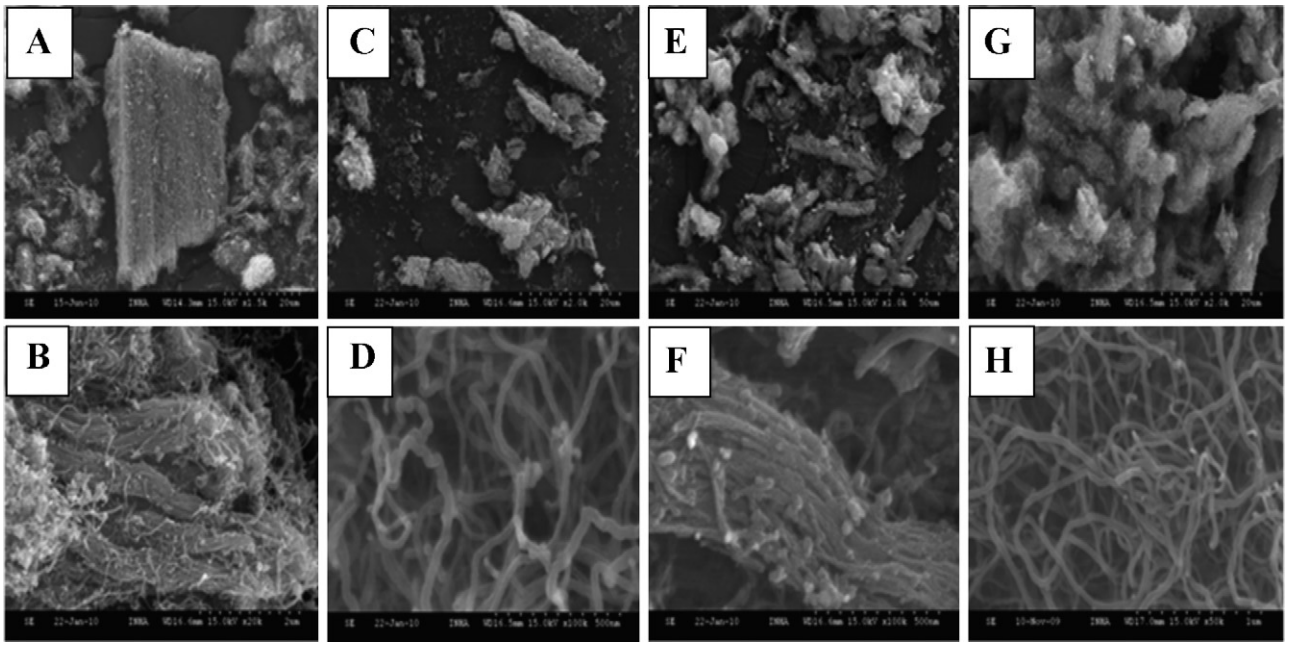

Fig. 2. SEM images of CNTs supported metal catalysts: CNTs-Co-10 at low magnification (A) and high magnification (B); CNTs-Co-30 at low magnification (C) and high magnification (D); CNTs-Ni-10 at low magnification (E) and high magnification (F); and CNTs-Ni-30 at low magnification (G) and high magnification (H).

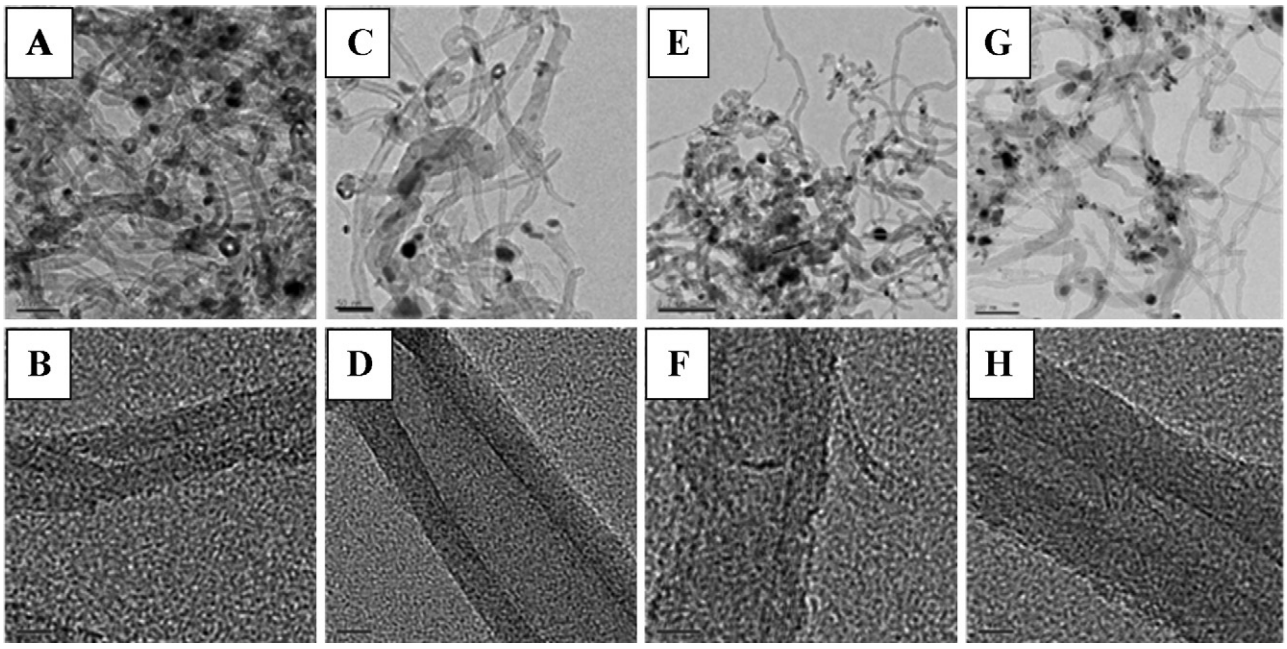

Fig. 3. TEM images of CNTs supported metal catalysts: CNTs-Co-10 at low magnification (A) and high magnification (B); CNTs-Co-30 at low magnification (C) and high magnification (D); CNTs-Ni-10 at low magnification (E) and high magnification (F); and CNTs-Ni-30 at low magnification (G) and high magnification (H).

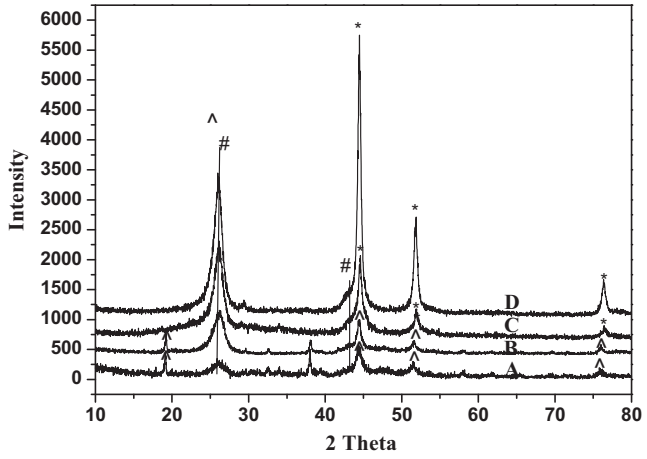

Fig. 4. Powder X-ray diffraction pattern of CNTs supported metal catalysts (CNTs: (#), Co (^) and Ni(*)): CNTs-Co-10 (A); CNTs-Co-30 (B); CNTs-Ni-10 (C) and CNTs-Ni-30 (D).

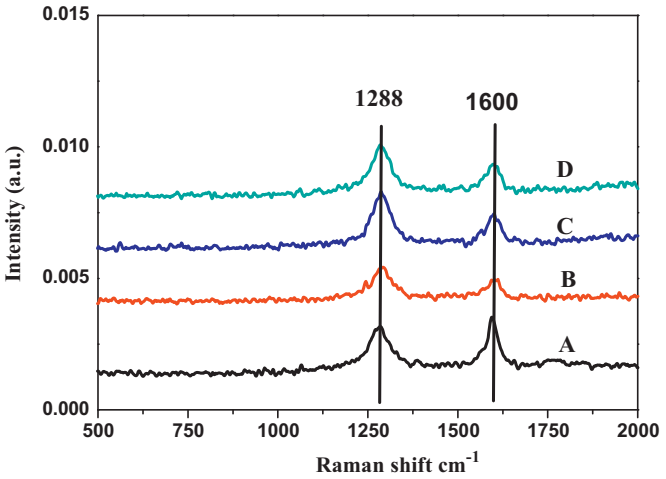

Fig. 5. Raman spectra of CNTs supported metal catalysts: CNTs-Co-10 (A); CNTs-Co-30 (B); CNTs-Ni-10 (C) and CNTs-Ni-30 (D).

metal particles on the surface of SBA-15 template. Big size particles in metal-CNTs were removed much easier than small one.

Table 2 shows the results of the catalytic activity during the dehydrogenation of ethylbenzene with various CNTs supported and metal-loaded activated carbon catalysts. The CNTs supported metal catalysts (Runs 6–8) exhibited a higher styrene yield and selectivity, ethylbenzene conversion than the metal-loaded activated carbon catalysts (Runs 3 and 4) and activated carbon (Run 2). It was due to the special structure of metal-CNTs. The CNTs supported Co and Co-loaded activated carbon catalyst exhibited a higher styrene yield and selectivity, ethylbenzene conversion than Ni loaded cat-

Table 1
Change of metal content in catalysts.[a]

Catayst	Amount of metal before NaOH treatment (wt% to SiO_2)	Amount of metal after NaOH treatment (wt% to carbon)
CNTs-Co-10	10	9.5
CNTs-Co-30	30	12.6
CNTs-Ni-10	10	9.3
CNTs-Ni-30	30	13.1

[a] Data obtained by SEM-EDX analysis.

Table 2
Dehydrogenation of ethylbenzene with various metal-loaded CNTs catalysts.[a]

Run	Catalyst	Metal (wt%)	EB conversion (%)	ST yield (%)	ST selectivity (%)
1	None	0	5.0	2.0	26.3
2	Ac	0	16.2	12.5	75.9
3	Co/Ac	10.0	61.3	54.6	64.6
4	Ni/Ac	10.0	55.6	52.7	55.8
5	CNTs	0	38.8	45.5	80.0
6	CNTs-Co-10	9.5	83.0	67.3	88.1
7	CNTs-Co-30	12.6	88.2	70.1	86.0
8	CNTs-Ni-10	9.3	72.0	62.0	83.1
9	CNTs-Ni-30	13.1	70.7	65.7	82.5

[a] Reaction temperature: 550 °C, catalyst weight 3 g and ethylbenzene/air = 1:600 (ml/min).

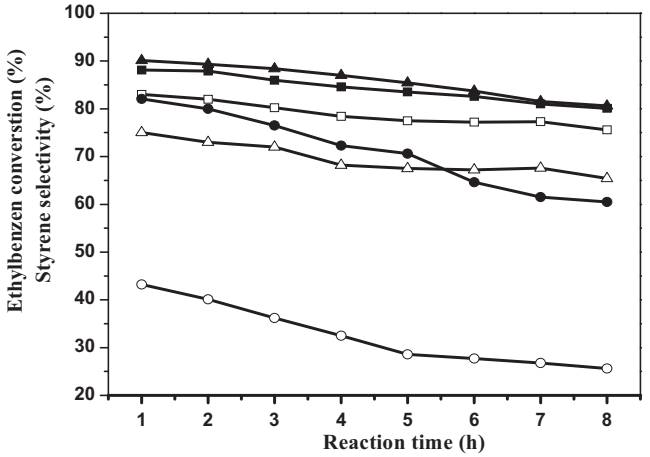

Fig. 6. Effect of oxidants on the conversion of ethylbenzene and selectivity of styrene (carbon dioxide (△), air (□) and argon (○)). Ethylbenzene conversion (open symbol) and styrene selectivity (solid symbol), reaction temperature: 1 h, 550 °C, catalyst (CNTs-Co-10) 3 g and ethylbenzene/oxidant = 1:600 (ml/min).

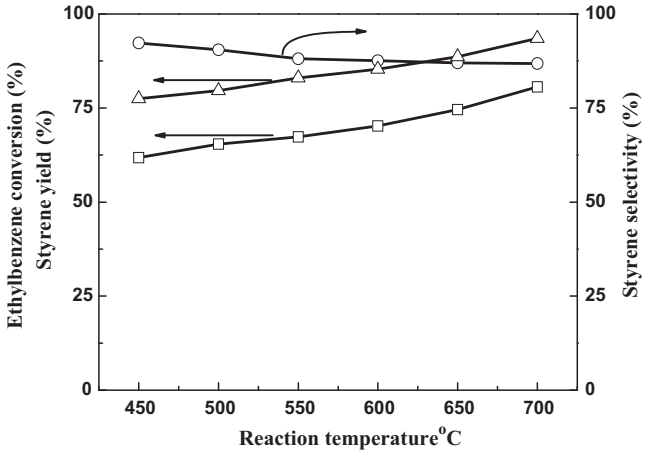

Fig. 7. Effect of reaction temperature on the conversion of ethylbenzene (△), yield (□) and selectivity (○) of styrene under air. Catalyst (CNTs-Co-10) 3 g and ethylbenzene/air = 1:600 (ml/min), 1 h.

alysts that were tested. Furthermore, styrene selectivity catalyzed by CNTs-Co-10 catalyst reached nearly 88.1% with 83% ethylbenzene conversion and 67.3% styrene yield. With increasing content of metals, ethylbenzene conversion and styrene yield were increased; however, selectivity of styrene was decreased.

Effect of different oxidants (carbon dioxide, air and argon) on the conversion of ethylbenzene and selectivity of styrene were investigated under reaction temperature (Fig. 6): 1 h, 550 °C, catalyst (CNTs-Co-10) 3 g and ethylbenzene/oxidant = 1:600 (ml/min). Carbon dioxide promoted high styrene selectivity (90.1%) of the dehydrogenation of ethylbenzene over CNTs-Co-10 catalyst because CO_2 is a mild oxidant. The Co catalyst exhibited high performance as regards the ethylbenzene conversion (83%) and styrene yield (67.3%) in the presence of air due to air strong oxidation.

The effect of the reaction temperature on the dehydrogenation of ethylbenzene with CNTs-Co-10 catalyst was examined. Ethylbenzene conversion, styrene yield, and selectivity as a function of reaction temperature are shown in Fig. 7 (under air flow). Ethylbenzene conversion increased from 77.5% at 450 °C to 93.5% at 700 °C. At the same time styrene yield increased from 61.8% at 450 °C to 80.6% at 700 °C. The styrene selectivity only decreased from 92.3% at 450 °C to 86.8 at 700 °C. Under the high temperature condition, styrene selectivity did not lead to a dramatic decrease in the air stream. In view of this finding, CNTs supported metal catalysts showed a very high thermal stability at a higher reaction temperature. This finding clearly indicates that bifunctional CNTs-supported Co or Ni catalyst gave the very high catalytic activity and a high thermal stability.

4. Conclusions

Different contents of CNTs-supported Ni and Co catalysts were synthesized by CVD method using SBA-15 as the template under methane and carbon dioxide. The catalysts were characterized by SEM, TEM, XRD, Raman and SEM-EDX. The catalytic activity was investigated for the dehydrogenation of ethylbenzene at different oxidants and temperatures. CNTs-Co-10 showed the highest styrene selectivity (92.3%) at 450 °C and ethylbenzene conversion (93.5%) at 700 °C with a higher styrene yield (80.6). The catalyst showed a high thermal stability.

References

[1] F. Cavani, F. Trifiro, Appl. Catal. A: Gen. 133 (1995) 219–239.
[2] A.L. Lisovskii, C. Aharon, Catal. Rev. Sci. Eng. 36 (1994) 25–74.
[3] W. Oganowski, J. Hanuza, L. Kepinski, Appl. Catal. A: Gen. 171 (1998) 145–154.
[4] G. Emig, H. Hofmann, J. Catal. 84 (1983) 15–26.
[5] M.F.R. Pereira, J.J.M. Órfão, J.L. Figueiredo, Appl. Catal. A: Gen. 184 (1999) 153–160.
[6] M.F.R. Pereira, J.J.M. Órfão, J.L. Figueiredo, Carbon 40 (2002) 2393–2401.
[7] G. Mestl, N.I. Maksimova, N. Keller, V.V. Roddatis, R. Schlögl, Angew. Chem. Int. Ed. 40 (2001) 2066–2068.
[8] D. Su, N. Maksimova, J.J. Delgado, N. Keller, G. Mestl, M.J. Ledoux, R. Schlögl, Catal. Today 102–103 (2005) 110–114.
[9] J.J. Delgado, R. Vieira, G. Rebmann, S. Su, N. Keller, M.J. Ledoux, R. Schlögl, Carbon 44 (2006) 809–812.
[10] N.M. Rodriguez, M.-S. Kim, R.T.K. Baker, J. Phys. Chem. 98 (1994) 13108–13111.
[11] M.F.R. Pereira, J.L. Figueiredo, J.J.M. Órfão, P. Serp, P. Kalck, Y. Kihn, Carbon 42 (2004) 2807–2813.
[12] O. Watzenberger, E. Ströfer, A. Anderlohr, Chem. Eng. Technol. 21 (1999) 659–662.
[13] W.Z. Li, S.S. Xie, L.X. Qian, B.H. Chang, B.S. Zou, W.Y. Zhou, R.A. Zhao, G. Wang, Science 274 (1996) 1701–1703.
[14] D.Y. Zhao, J.L. Feng, Q.S. Huo, N. Melosh, G.H. Fredrickson, B.F. Chmelka, G.D. Stucky, Science 279 (1998) 548–552.